Highly transparent, stretchable, and self-healing ionic-skin triboelectric nanogenerators for energy harvesting and touch applications

Parida, Kaushik; Kumar, Vipin; Wang, Jiangxin; Bhavanasi, Venkateswarlu; Bendi, Ramaraju; Lee, Pooi See

2017

Parida, K., Kumar, V., Wang, J., Bhavanasi, V., Bendi, R., & Lee, P. S. (2017). Highly transparent, stretchable, and self-healing ionic-skin triboelectric nanogenerators for energy harvesting and touch applications. Advanced Materials, 29(37), 1702181-. doi:10.1002/adma.201702181

https://hdl.handle.net/10356/140427

https://doi.org/10.1002/adma.201702181

WILEY-VCH

DOI: 10.1002/((please add manuscript number))
Article type: Communication

Highly Transparent, Stretchable and Self-healing Ionic Skin Triboelectric Nanogenerators for Energy Harvesting and Touch Panels

*Kaushik Parida, Vipin Kumar, Wang Jiangxin, Venkateswarlu Bhavanasi, Ramaraju Bendi and Pooi See Lee**

Kaushik Parida, Vipin Kumar, Wang Jiangxin, Venkateswarlu Bhavanasi, Ramaraju Bendi and Pooi See Lee*

School of Materials Science and Engineering, Nanyang Technological University,

50 Nanyang Avenue, Singapore 639798

Phone: (+65) 6790-6661

Fax: (+65) 6790-9081
E-mail: pslee@ntu.edu.sg

Keywords: Triboelectric, Nanogenerator, Stretchable, Self-healing, Transparent

Abstract

Recently developed triboelectric nanogenerators (TENGs) act as a promising power source for self-powered electronic devices. However, majority of the TENGs are fabricated using metallic electrodes that could not achieve high stretchability and transparency, simultaneously. In this work, slime-based ionic conductors are used as transparent current-collecting layers of TENG, thus significantly enhancing their energy generation, stretchability, transparency, and instilling self-healing characteristics. This work is the first demonstration of ionic conductor as the current collector in a mechanical energy harvester. The resulting ionic skin TENG (IS-TENG) has a transparency of 92% transmittance, and its energy harvesting performance is 12 times

higher than that of the silver-based electronic current collectors. In addition, they are capable of enduring a uniaxial strain up to 700%, giving the highest performance compared to all the transparent and stretchable mechanical energy harvester. Additionally, this is the first demonstration of an autonomously self-healing TENG which can recover its performance even after 300 times of complete bifurcation. Our IS-TENG represents the first prototype of highly deformable and transparent power source that is able to autonomously self-heal quickly and repeatedly at room temperature, and thus can be used as power supplies for digital watches, touch sensors, artificial intelligence and bio-integrated electronics.

1. Introduction

The emergence of next-generation electronics or bioelectronics has propelled immense enthusiasm for the development of various deformable, transparent, and self-healable electronic devices, including transistors,[1,2] strain sensors,[3,4] energy storage devices,[5–7] and light-emitting diodes (LEDs).[8,9] In particular, deformable devices that can be conformally integrated on arbitrary, irregular, and movable surfaces without deterioration of their performance are currently in high demand.[10,11] Additionally, the ability of a device to restore its functionality after mechanical damage is crucial for the realization of highly durable electronics,[12] while transparency helps in the visual transmission of information, which can be potentially utilized in user-interactive displays, biomedical imaging, therapeutic optogenetics and touch screens.[13,14] However, powering the described next-generation electronic devices requires sustainable power source characterized by integrated stretchability, transparency, and self-healability properties.

Recently, triboelectric nanogenerators (TENGs) reported by Wang et al. have been utilized as power source for self-powered electronics due to their high voltage output, ability to function

at very low and irregular mechanical impulses, high efficiency, easy availability, environmental friendliness, and low processing costs.[15–18] However, most of the currently used TENGs contain metallic electrodes and therefore lack sufficient transparency, stretchability, and self-healing characteristics.[19,20] Serious efforts have been made to develop highly deformable TENGs by improving their design and fabrication procedure.[21–24] For example, serpentine-patterned electrodes and interlocking Kirigami structures were used; however, the maximum tensile strains of the resulting TENGs were limited to 22% and 100%, respectively, due to the traditional planar structural design and material strain limitation.[22,23] Embedding metallic conductors into a stretchable matrix (such as Ag nanowires[24] and carbon black[21] in silicone rubber) resulted in the remarkable ability of the fabricated TENGs to sustain their performance at extreme deformations (corresponding to uniaxial strains of up to 300%). However, the use of opaque current collectors limits both the device transparency and stretchability. Despite attempts to fabricate self-healing TENGs from thermally induced shape-memory polymers, the produced devices required thermal activation for the self-healing process and lacked sufficient stretchability and transparency.[25] Therefore, the key challenge is to fabricate TENGs with various incorporated functionalities (including stretchability, transparency, and self-healability), which can be easily integrated with multiple functions for non-conventional applications.

In this work, extremely stretchable, highly transparent, and self-healing ionic skin triboelectric nanogenerators (IS-TENGs) for powering electronic devices and touch sensor applications have been fabricated using slime-based ionic conductors as the current collector. To the best of our knowledge, this is the first demonstration of ionic conductors as the current collector in mechanical energy harvesters. The use of ionic conductor significantly enhances the energy harvesting performance due to the formation of an electrical double layer (EDL). Owing to the non-Newtonian behavior of the current collector, an extreme stretchability as high as 700% was

achieved without degrading the device performance, which enables the IS-TENG as a power source for highly deformable electronics. The performance of the device under multiple stretching cycles was evaluated. The dynamic hydrogen bonds of the ionic conductor resulted in an autonomous self-healing IS-TENG. The energy harvesting performance of the fabricated IS-TENGs was evaluated after inflicting multiple mechanical damages. The practical applicability of the IS-TENG was demonstrated by charging a commercial dielectric capacitor as well as by powering a digital watch and LEDs. Furthermore, a highly stretchable, self-healing, and transparent touch screen for computing operation has been demonstrated in this study.

2. Results and Discussion

Figure 1a shows the schematic of the fabricated IS-TENG, which consists of a silicone rubber layer with a thickness of 100 ± 10 μm, utilized as the triboelectrically negative material, a slime layer (a cross-linked poly(vinyl alcohol) (PVA) gel) with a thickness of 1 mm, as the ionic current collector, and VHB tape with a thickness of 1 mm as a substrate. Figure 1b shows the digital photograph of the highly transparent IS-TENG, its detailed fabrication method is described in the Experimental sections and Supporting Information, Figure S1. Silicone rubber is generally considered a good triboelectrically negative material due to its high electronegativity and the potential ability to generate large triboelectric charges upon contact with human skin[24,26] (it should be noted that human skin and silicone rubber correspond to the positive and negative ends of the triboelectric series, respectively). Silicone rubber has been used in various TENGs as a functional dielectric,[24,26] stretchable substrate,[26,27] and encapsulation material,[21,28] owing to its excellent stretchability, superior tear strength, and low Young's modulus. Figure S2, Supporting Information shows the digital photograph of the highly transparent slime layer (100% transmittance for visible light, Figure 1c), which was formed due to the weak hydrogen bonding interactions between the tetrafunctional borate ions

with the –OH group of PVA, as illustrated in Figure S3, Supporting Information). The presence of the hydrogen bonding is verified from the Fourier transform infrared spectroscopy (FTIR) (Figure S4). The subsequent cross-linking led to the formation of a three-dimensional (3D) polymer network.[29] The produced slime exhibited high ionic conductivity (2.9×10^{-5} Scm^{-1}) due to the presence of positive (Na^+) and negative ions ($B(OH)_4^-$), which was measured using electrochemical impedance spectroscopy (EIS) (Figure 1f). The 3D PVA network provided the necessary path for ion transport (it was selected as the polymer matrix due to its non-toxicity, biocompatibility, high transparency, and high ionic conductivity[30]). The produced weak bonds led to the formation of a viscoelastic non-Newtonian fluid;[31] as a result, the slime layer could be stretched by progressive pulling and assumed the shape of a mold or container. The self-healing properties of the slime layer originated from the weak hydrogen bonding interactions.[29] The commercial VHB adhesive tape (used as the substrate) was transparent, stretchable, and self-healing. Thus, the resulting IS-TENG exhibits superior transparency, stretchability, and self-healing characteristics. Figure 1e shows the digital photographs of the fabricated IS-TENG that was subjected to various mechanical deformations, such as uniaxial stretching up to 700% strain as well as folding and rolling. The resulting IS-TENG exhibited 92% transmittance for visible light, measured in the wavelength range of 300 – 900 nm (Figure 1c). All the utilized materials were inexpensive and easily processable, which ensured high scalability and industrial adaptability of the fabricated devices.

2.1. Mechanism of energy generation

Figure 1d schematically illustrates the mechanism of the IS-TENG operation. In particular, the energy generation occurs due to the coupling between the triboelectric and electrostatic induction effects.[15,24,32] According to the triboelectric series, human skin can be considered an excellent triboelectrically positive material (due to its relatively low electronegativity), and silicone rubber represents an excellent triboelectrically negative material (due to its relatively

high electronegativity).[24] Initially, the surfaces of silicone rubber and human skin were not in contact and therefore generated no surface charges; as a result, the positive (Na^+) and negative ($B(OH)_4^-$) ions of the ionic conductor remains randomly distributed across the PVA matrix. When the human skin comes in contact with the silicone rubber layer, charge transfer from the human skin to the rubber (due to the difference in their electronegativities), making the silicone rubber negatively charged, and the human hand positively charged.[24] When the finger is moved away from the surface, the two oppositely charged surfaces (human skin and silicone rubber) become separated in space, thus creating a potential difference. The unscreened negative charge on the surface of silicone rubber induces the accumulation of positive ions (Na^+) at the silicone rubber/slime interface and negative ions ($B(OH)_4^-$) at the slime/copper interface, which in turn leads to electrical double layer formation.[33] This leads to a transient charge flow from the copper electrode to the ground, generating a voltage output. An electrostatic equilibrium is achieved when the two oppositely charged surfaces reach the maximum separation distance. When the mechanical force is applied again, the distance between the skin and the silicone rubber layer as well as their potential difference decreases, resulting in a charge flow in the opposite direction (from the ground to the slime/copper interface), which generates a voltage in the reverse direction.[16,34] Thus, repeating the procedure described above produces multiple voltage outputs.

2.2. Energy harvesting performance of IS-TENGs

The energy harvesting performance of the fabricated IS-TENG (represented by the open-circuit voltage (V_{oc}), short-circuit current density (I_{sc}), and charge transfer density (σ_T)) was evaluated by applying a compressive mechanical force of approximately 10 N via finger tapping at a frequency of 4 Hz, similar to the testing procedure utilized for other skin-based TENGs.[24,26,35–38] The IS-TENG generated the approximate V_{oc} of 50 V (Figure 2a), I_{sc} of 6.5 $\mu A \cdot cm^{-2}$ (Figure

2b), and σ_T of 17 nC·cm^{-2} (Figure 2c). The application of a mechanical force produces a positive voltage peak, while its release generates a negative peak. During practical application, the IS-TENG can be subjected to mechanical force of various magnitude, the corresponding responses of the device under various mechanical forces were evaluated. Figure S5 Supporting Information, shows the voltage output, current density, and charge transfer when subjected to different magnitude of applied force. When the magnitude of the applied force increases, the effective contact area between the silicone rubber and the human skin increases, thus enhancing the energy harvesting performance of the fabricated IS-TENG. The impedance of the load affects the performance of the energy harvesting device. Hence, the energy harvesting performance of the IS-TENG was evaluated across various load resistance. Figure 2d shows the variations of the voltage output and current density of the fabricated IS-TENG with different load resistance. Due to Ohm's law, the output voltage increases and the output current decreases with an increase in the load resistance. Figure 2e shows the variation of the power density (defined by the formula P = V·I, where P is the power density, V is the output voltage across the external load, and I is the output current density across the external load) with different load resistance. According to the maximum power transfer theorem, a maximum power density of 40 μW·cm^{-2} was obtained across an external load resistance of 1 MΩ. The stability of the produced IS-TENG was evaluated by measuring the voltage output for 1000 continuous cycles with an interval of 15-days (Figure 2f). The device showed stable performance even after 15 days, indicating the durability of the device. The detailed stability analysis of the IS-TENG is provided in the supporting information (Figure S20 and S21).

For comparison purposes, the energy harvesting performance of the control sample (a TENG utilizing a silver electrode as the current collector) was evaluated as well (Figure S6, Supporting Information, shows the schematic of the control sample). It consisted of the silicone rubber layer with a thickness of 100 ± 10 μm and area of 2 × 2 cm^2 and the silver paste layer with an

area of 1 × 1 cm^2, and sheet resistance of 4 Ωcm^{-1}. The control sample generated approximate V_{oc} of 11 V, I_{sc} of 2 $\mu A \cdot cm^{-2}$, and σ_T of 3 $nC \cdot cm^{-2}$ upon finger tapping at an approximate force of 10 N at a frequency of 4 Hz (Figure S7, Supporting Information). The power density generated across the load resistance of 1 MΩ was 3.3 $\mu W \cdot cm^{-2}$ (Figure S7d). Thus, the IS-TENG with an ionic current collector exhibited a 12-fold enhancement in the power density as compared to that generated by the control sample. The observed enhancement in the energy harvesting performance for the IS-TENG with an ionic conductor can be attributed to the EDL formation. The magnitude of V_{oc} of the IS-TENG depends on the triboelectric charge density on the silicone rubber surface, which in turn depends on the device capacitance.[39,40] Thus, a higher capacitance leads to a higher output voltage. During voltage generation, the positive and negative ions of the slime form an EDL at the slime/silicone rubber and slime/copper interfaces, respectively. The EDL charge separation distance is infinitesimally small (in few nanometers), which significantly increases the capacitance of the device with an ionic conductor (Figure S8; shows the capacitance of the slime and the silicone rubber as a function of frequency). As a result, the output performance of the fabricated IS-TENG (which is directly related to the device capacitance) increases, indicating that the use of the slime-based ionic conductor as a current collector can significantly improve its energy harvesting performance. The voltage generated from the IS-TENG with only PVA (without inclusion of ions) is lower compared to the device with slime layer, due to the lower capacitance (Figure S9). The variation of power density of the IS-TENG as a function of the capacitance of the ionic conductor further validates the hypothesis (Figure S10). Ionic conductors have been used in electronic devices such as actuators,[41,42] electroluminescent (EL) devices,[43–45] and touch sensors.[13,14,46] However, to the best of our knowledge this is the first demonstration of the use of an ionic conductor as the current collector in an energy harvesting device. Comparison of the energy harvesting performance of the IS-TENG with other mechanical energy harvesters are provided in Table S1 and S2, supporting information.

To realize deformable self-powered electronics, the fabricated TENG must be able to maintain its functionality under extreme deformation. Hence, the performance of the fabricated IS-TENG was evaluated in this study under extreme deformation conditions such as uniaxial stretching as well as folding and rolling (Figure 1e). Its energy harvesting performance was measured at different uniaxial strains between 0 and 700% (calculated using the formula $(L_E - L_i)/ L_i \times 100\%$), where L_E was the elongated length, and L_i was the initial device length). Figure 3a and b shows the variation of voltage output and current density (generated by finger tapping on the IS-TENG at an approximate force of 10 N and frequency of 4 Hz) at various uniaxial strains. The statistical data is obtained form 3 devices, for 4 cycles of voltage output. Figure 3c shows the voltage response of the IS-TENG at 700 % strain. The obtained results indicate that the voltage and current output increases with an increase in the axial strain. The increase in the output performance can be attributed to the decrease in the thickness of the dielectric layer upon stretching, due to Poisson's effect. This enhances the device capacitance, thus increasing the surface charge density. As a result, the voltage output increases with an increase in the surface charge density. The increase in the uniaxial strain increases the ionic resistance of the slime layer (Figure S11, Supporting Information). Therefore, the improved energy harvesting performance of the IS-TENG can be attributed to the dominating effect of the reduction in the thickness of the dielectric layer. When the IS-TENG was restored to the original unstrained condition, it generated a voltage output of approximately 50 V at similar conditions (which was close to the voltage measured before stretching, see Figure S12), indicating that the produced device could effectively return to its original state after extreme deformation. The observed phenomenon can be explained by the presence of the slime-based ionic conductor, which possesses the ability to easily recover after severe mechanical deformations and restore its initial ionic conductivity. Hence, the fabricated IS-TENG can be potentially used as a power supply for deformable electronics. The IS-TENG showed stable performance for 500 cycles of

dynamic stretching (Figure 3d). The voltage output was measured after every 50 cycles of dynamic stretching. The statistical data is obtained from 5 cycles of voltage output. Furthermore, upon folding (as seen from Figure 1e), the device generates a voltage of approximately 50 V upon finger tapping at a force of 10 N and frequency of 4 Hz. Additionally, upon rolling (as seen in Figure 1e), the device generates a voltage of approximately 50 V under similar experimental conditions.

During real-time operation, the TENG can undergo mechanical damage due to deformation, wear and tear, and accident inflicts. Hence, the realization of a robust and sustainable self-healing energy harvester includes the ability to restore its performance after extreme mechanical damage. Thus, the performance of the fabricated IS-TENG was measured after subjecting the device to extreme mechanical damage, such as complete bifurcation and quadifurcation of the device. After the fabricated IS-TENG was completely bifurcated, it managed to completely heal itself without applying any external stimuli (Figure 4a). Energy harvesting performance of the bifurcated devices (corresponding to the voltage output of around 50 V generated upon finger tapping at an approximate force of 10 N and frequency of 4 Hz) was monitored before and after self-healing (Figure 4b, Supporting Information). Subsequently, the IS-TENG was quadrifurcated (Figure 4a), its energy harvesting performance was completely restored after self-healing (Figure 4b). The durability of the fabricated IS-TENG was further evaluated by measuring its energy harvesting performance under similar conditions for 300 cycles of bifurcation and self-healing at the same location; as a result, no significant decrease in the voltage output was observed (Figure 4c). The voltage output was measured after every 50 cycles of bifurcation and self-healing. The statistical data is obtained from 5 cycles of voltage output. The obtained results indicate that the fabricated IS-TENG exhibits sustainable durability and is capable of retaining the original performance with quick recovery after undergoing cyclic mechanical damage. During the self-healing process, the device restores both its mechanical

and electrical properties; thus, the slime layer recovers its original ionic conductivity within the first 32 s with an efficiency of 99% (more details are provided in the Supporting Information section, Figure S13). The observed self-healing process of the produced IS-TENG can be attributed to the presence of both the slime-based current collector and VHB tape. Slime possesses self-healing property due to the weak hydrogen bonding interactions between its tetrafunctional borate ions and –OH groups, which are schematically illustrated in Figure S14, Supporting Information. The cross-linked polymer network remains in a state of dynamic equilibrium, where weak bonds can be easily disrupted and restored at room temperature without application of any external stimuli. Pioneering work on stretchable and self-healing materials were reported by Moore and co-workers by incorporating mechanophores.[47–49] They demonstrated by using mechanophores as cross-linkers or by linking them with polymer chains, highly mechanoresponsive materials can be fabricated. In previous studies of self-healing TENGs, the self-healing process of pyramidal structural degradation was demonstrated by using shape memory polymers.[25] However, the resulting device failed to exhibit self-healing properties after complete bifurcation, and its full restoration required thermal treatment. To the best of our knowledge, this work represents the first demonstration of an autonomous self-healing TENG with a significantly prolonged lifespan, which can be potentially utilized in prosthetic and wearable electronics. Additional discussions on the self-healing behavior of the IS-TENG is provided in the supporting information (Figure S22, S23 and S24). Detailed mechanical properties (including mechanical properties before and after healing, healing time, and healing efficiency) of the self-healing behavior of the slime based ionic current collector is provided in the supporting information (Figure S25, S26, S27, S28 and S29).

The ability of the IS-TENG to generate superior energy harvesting performance, while being extremely deformable, highly transparent and autonomously self-healing makes it an ideal power source for the realisation of self-powered electronics and touch screen. The IS-TENG

can be used directly to drive external load for real-time applications. This feature was demonstrated by powering up commercial LEDs. A pack of 40 LEDs were powered by the IS-TENG (active device area of 1 × 1 cm^{-2}, attached to the back of human hand) by palm tapping (Figure 5d, S13 and as demonstrated in Video 1, Supporting Information). The circuit diagram is illustrated in Figure S16a, Supporting Information. The ability of IS-TENG to perform under extreme deformation was further explored by powering up LEDs by palm tapping on the IS-TENG stretched at 600 % axial strain (Figure 5e, S15 and as ddemonstrated in Video 2, Supporting Information). Furthermore, the self-healing ability of the IS-TENG, was explored by powering up LEDs after extreme mechanical damage. To demonstrate this, the IS-TENG was attached to a fabric. The fabric with device was cut into two parts and then joined physically. Upon self-healing, the device could power a pack of 40 LEDs upon palm tapping (Figure 5f, S16 and as demonstrated in Video 3, Supporting Information). This demonstration shows that the IS-TENG sustain its performance after severe mechanical damage thus significantly extending the lifetime of electronics devices. The energy generated from the IS-TENG can be stored, to power up electronic devices for self-powered device application. To demonstrate this capability, a commercial dielectric capacitor (10 μF) was charged by finger tapping on the IS-TENG (Figure S19, Supporting Information). The energy stored in the capacitor was used to drive a digital watch. Figure 5c shows the digital photo of the charging of a digital watch by IS-TENG (held onto the user's palm). The detailed circuit diagram is illustrated in Figure S16b, Supporting Information. The digital watch starts working when the stored energy in the capacitor is enough to power the digital watch. The demonstration is shown in Video 4, Supporting Information. The charging of digital watch by our IS-TENG paves the path for the realisation of truly self-powered electronic devices. Furthermore, we demonstrated the use of IS-TENG as a deformable, transparent, autonomously self-healing epidermal touch panel (Figure 5a, b and Video 5, Supporting Information). The IS-TENG was connected to a computer through a microcontroller. The voltage output generated from the IS-TENG upon

palm tapping was fed to the controller. The microcontroller was programmed to detect the signals from the IS-TENG and control the computer. The device can be directly integrated onto any part of the human body regardless of its physical dimensions, shape and conformability, for the realisation of an epidermal touch sensors.

3. Conclusions

In conclusion, a disruptive technology of slime-based ionically conducting current collectors for TENG is demonstrated for the first time, which enhances its energy harvesting performance due to the formation of an electrical double layer and facilitates additional functionalities such as stretchability, transparency, and self-healing properties. Owing to the transparent nature of the current collector, the fabricated IS-TENG exhibited a transparency of 92%, thus paving the way for its use as a power supply for transparent electronics devices. In addition, the fabricated IS-TENG was characterized by remarkable energy harvesting performance under extreme deformations such as uniaxial strains of up to 700% and sustained its energy harvesting performance after 500 dynamic cycles of stretching, indicating its high durability under extreme deformation conditions. Additionally, the fabricated device demonstrates self-healing properties and was able to recover its energy harvesting performance after 300 cycles of repetitive mechanical damage. Owing to the combination of the transparency and stretchability properties as well as the ability to autonomously self-heal at room temperature, the fabricated IS-TENG takes a quantum leap in the domain of deformable mechanical energy harvester. The applicability of the designed IS-TENG as a sustainable energy source for self-powered electronics was demonstrated by powering commercial LEDs, digital watch and skin-based touch screens. Hence, the scientific innovative concept and disruptive technology demonstrated in this work open up new possibilities for the utilization of TENGs for a broad spectrum of application including health monitoring, sports, wearable and implantable electronics, and smart robotics, enabling a huge step towards the realization of next-generation electronics.

4. Experimental Section

Fabrication of slime (ionic conductor) and silicone rubber:

Poly (vinyl alcohol) (average Mw 130,000, >99% hydrolyzed, Sigma-Aldrich), Sodium tetraborate (Sigma-Aldrich) were used as received without further purification. The 10 wt % PVA solution was prepared by slowly adding PVA powder to DI water maintained at a temperature of 80 ^{o}C while stirred vigorously. Slow adding ensures individual wetting of polymer grains. A viscous and clear solution was obtained after 3 h of stirring at 80 ^{o}C. 4 wt % borax solution was separately prepared by mixing hydrated sodium tetraborate ($Na_2B_4O_7.10H_2O$) in DI water. Borax solution was added to the PVA solution in a mixture of 10:1 (PVA:borax) volumetric ratio, while vigorously stirring with a spatula until the mixture was complete gelled. The reason of using 10:1 volumetric ratio of PVA:borax is explained in the supporting information. The obtained slime is transparent and viscous. The air bubbles were removed by leaving the slime to settle for 2 days.

The silicone rubber was fabricated by spin coating a well-mixed mixture of commercial available Ecoflex 00-50 part A and part B (in a weight ratio of 1:1) on a glass slide. It was cured at room temperature for 2 h. The freestanding silicone rubber was obtained by peeling off the film from the glass slide.

Fabrication of the IS-TENG:

Figure S1, schematically illustrates the detailed fabrication process of the IS-TENG. The IS-TENG consist of slime sandwich between silicone rubber and VHB tape. VHB tape (VHB 4010, 3M, USA) was used as the substrate (area = 2 × 2 cm^{-2}, thickness = 1 mm). A conducting wire was attached to the substrate as shown in Figure S1. To ensure proper encapsulation and sealing of the slime, a cavity (area = 1 × 1 cm^2, thickness = 1 mm) was made by sticking one more layer of VHB tape (with a rectangular hole in the centre) onto the substrate. The adhesive of the VHB tape ensures proper sealing. Slime was drop casted onto the cavity, with a controlled

thickness of 1 mm. Subsequently, silicone rubber (area = 2 × 2 cm^{-2}, thickness = 100 ± 20 μm, prepared by spin coating) was attached at the top of slime. The adhesive of the VHB tape ensure good adhesion between the silicone rubber and the VHB tape. The inherent adhesive of the VHB tape ensures proper encapsulation and sealing, which prevents the slime from drying up. To fabricate the control sample (Figure S6, Supporting Information), silver paste (area = 1 × 1 cm^2 and sheet resistance = 4 Ωcm^{-1}) was applied on the freestanding silicone rubber (area = 2 × 2 cm^{-2}, thickness = 100 ± 20 μm, prepared by spin coating). Copper tape was used to connect the silver paste to the measuring instrument.

Characterization:

The thickness of spin-coated silicone rubber, VHB tape and slime was measured using screw-gauge. Shimadzu spectrometer (UV-2501pc,) was used to measure the transmittance spectra of the materials and the IS-TENG with respect to a glass slide over the range of 300 to 900 nm. The device was stretched using a home-built stretching stages. The force exerted on the fabricated device was measured by the Force gauge (Sinocera, Model CL-YD-303). The output voltage from the TENG were measured using an oscilloscope (Trektronix, MDO 3024, impedance = 10 MΩ), the output current was measured using a low noise current pre-amplifier (Stanford Research System, Model SR570, impedance = 4 Ω) and the charge transfer was measured using a electromter (Keithley 6514 system electrometer, input resistance = 200 TΩ). The Fourier transform infrared spectroscopy was done using FTIR-ATR (Perkin Elmer Frontier). The electrochemical impedance spectroscopy of the slime was measured using a potentiostat (Autolab PGSTAT 30), by sandwiching the slime layer (area = 1 × 1 cm^{-2}, thickness = 1 mm) between two Indium Tin Oxide (ITO) glass pieces. The sheet resistance of the silver electrode (of the control sample) was measured using a four-probe resistance measurement system (Advance Instrument Technology, CMT-SR2000N). A LCR meter (Agilent E4980A Precision), was used to measure the capacitance and resistance of the slime at various

experimental conditions. The capacitance of the slime (ionic conductor) and silicone rubber was measured at a voltage of 0.1 V applied over a frequency range, by sandwiching the materials between two ITO glass pieces. The resistance change of the slime at various strain was measured (using the LCR meter) by inserting two metallic wire at the two-extreme end of the IS-TENG. The change in the resistance of the slime (ionic conductor) during bifurcation and self-healing was measured (using the LCR meter), by inserting two metallic wire at the two-extreme end of the IS-TENG.

Supporting Information

Supporting Information is available from the Wiley Online Library or from the author.

Acknowledgements

This work is supported by the National Research Foundation Investigatorship, Award No. NRF-NRFI2016-05 and NRF Competitive Research Programme, Award No. NRF-CRP-13-2014-02. Kaushik Parida acknowledges the research scholarship provided by Nanyang Technological University, Singapore.

Received: ((will be filled in by the editorial staff))
Revised: ((will be filled in by the editorial staff))
Published online: ((will be filled in by the editorial staff))

Reference

[1] J. Y. Oh, S. Rondeau-Gagné, Y.-C. Chiu, A. Chortos, F. Lissel, G.-J. N. Wang, B. C. Schroeder, T. Kurosawa, J. Lopez, T. Katsumata, J. Xu, C. Zhu, X. Gu, W.-G. Bae, Y. Kim, L. Jin, J. W. Chung, J. B.-H. Tok, Z. Bao, *Nature* **2016**, *539*, 411.

[2] M. Kaltenbrunner, T. Sekitani, J. Reeder, T. Yokota, K. Kuribara, T. Tokuhara, M. Drack, R. Schwodiauer, I. Graz, S. Bauer-Gogonea, S. Bauer, T. Someya, *Nature* **2013**, *499*, 458.

[3] B. C.-K. Tee, C. Wang, R. Allen, Z. Bao, *Nat Nano* **2012**, *7*, 825.

[4] X. Huang, Y. Liu, H. Cheng, W.-J. Shin, J. A. Fan, Z. Liu, C.-J. Lu, G.-W. Kong, K. Chen, D. Patnaik, S.-H. Lee, S. Hage-Ali, Y. Huang, J. A. Rogers, *Adv. Funct. Mater.* **2014**, *24*, 3846.

[5] S. Xu, Y. Zhang, J. Cho, J. Lee, X. Huang, L. Jia, J. A. Fan, Y. Su, J. Su, H. Zhang, H. Cheng, B. Lu, C. Yu, C. Chuang, T. Kim, T. Song, K. Shigeta, S. Kang, C. Dagdeviren, I. Petrov, P. V Braun, Y. Huang, U. Paik, J. A. Rogers, *Nat. Commun.* **2013**, *4*, 1543.

[6] Y. Huang, M. Zhong, Y. Huang, M. Zhu, Z. Pei, Z. Wang, Q. Xue, X. Xie, C. Zhi, *Nat. Commun.* **2015**, *6*, 10310.

[7] K. Parida, V. Bhavanasi, V. Kumar, J. Wang, P. S. Lee, *J. Power Sources* **2017**, *342*, 70.

[8] T. Someya, *Nat Mater* **2010**, *9*, 879.

[9] J. Liang, L. Li, X. Niu, Z. Yu, Q. Pei, *Nat Phot.* **2013**, *7*, 817.

[10] T. Sekitani, Y. Noguchi, K. Hata, T. Fukushima, T. Aida, T. Someya, *Science.* **2008**, *321*, 1468.

[11] D.-Y. Khang, H. Jiang, Y. Huang, J. A. Rogers, *Science.* **2006**, *311*, 208.

[12] A. Chortos, J. Liu, Z. Bao, *Nat Mater* **2016**, *15*, 937.

[13] J.-Y. Sun, C. Keplinger, G. M. Whitesides, Z. Suo, *Adv. Mater.* **2014**, *26*, 7608.

[14] C.-C. Kim, H.-H. Lee, K. H. Oh, J.-Y. Sun, *Science.* **2016**, *353*, 682.

[15] Z. L. Wang, J. Chen, L. Lin, *Energy Environ. Sci.* **2015**, *8*, 2250.

[16] S. Wang, L. Lin, Z. L. Wang, *Nano Energy* **2015**, *11*, 436.

[17] J. Chun, B. U. Ye, J. W. Lee, D. Choi, C.-Y. Kang, S.-W. Kim, Z. L. Wang, J. M. Baik, *Nat. Commun.* **2016**, *7*, 12985.

[18] J. Bae, J. Lee, S. Kim, J. Ha, B.-S. Lee, Y. Park, C. Choong, J.-B. Kim, Z. L. Wang, H.-Y. Kim, J.-J. Park, U.-I. Chung, *Nat. Commun.* **2014**, *5*, 4929.

[19] J. Wang, S. Li, F. Yi, Y. Zi, J. Lin, X. Wang, Y. Xu, Z. L. Wang, *Nat. Commun.* **2016**, *7*, 12744.

[20] K. N. Kim, J. Chun, J. W. Kim, K. Y. Lee, J.-U. Park, S.-W. Kim, Z. L. Wang, J. M. Baik, *ACS Nano* **2015**, *9*, 6394.

[21] F. Yi, J. Wang, X. Wang, S. Niu, S. Li, Q. Liao, Y. Xu, Z. You, Y. Zhang, Z. L. Wang, *ACS Nano* **2016**, *10*, 6519.

[22] P.-K. Yang, L. Lin, F. Yi, X. Li, K. C. Pradel, Y. Zi, C.-I. Wu, J.-H. He, Y. Zhang, Z. L. Wang, *Adv. Mater.* **2015**, *27*, 3817.

[23] C. Wu, X. Wang, L. Lin, H. Guo, Z. L. Wang, *ACS Nano* **2016**, *10*, 4652.

[24] Y.-C. Lai, J. Deng, S. Niu, W. Peng, C. Wu, R. Liu, Z. Wen, Z. L. Wang, *Adv. Mater.* **2016**, *28*, 10024.

[25] J. H. Lee, R. Hinchet, S. K. Kim, S. Kim, S.-W. Kim, *Energy Environ. Sci.* **2015**, *8*, 3605.

[26] S. Li, W. Peng, J. Wang, L. Lin, Y. Zi, G. Zhang, Z. L. Wang, *ACS Nano* **2016**, *10*, 7973.

[27] X. He, Y. Zi, H. Guo, H. Zheng, Y. Xi, C. Wu, J. Wang, W. Zhang, C. Lu, Z. L. Wang, *Adv. Funct. Mater.* **2017**, 4, 1604378.

[28] H. Guo, M.-H. Yeh, Y.-C. Lai, Y. Zi, C. Wu, Z. Wen, C. Hu, Z. L. Wang, *ACS Nano* **2016**, *10*, 10580.

[29] E. Z. Casassa, A. M. Sarquis, C. H. Van Dyke, *J. Chem. Educ.* **1986**, *63*, 57.

[30] A. A. Mohamad, N. S. Mohamed, M. Z. A. Yahya, R. Othman, S. Ramesh, Y. Alias, A. K. Arof, *Solid State Ionics* **2003**, *156*, 171.

[31] V. de Zea Bermudez, P. P. de Almeida, J. F. Seita, *J. Chem. Educ.* **1998**, *75*, 1410.

[32] Z. L. Wang, *Faraday Discuss.* **2014**, *176*, 447.

[33] B. U. Ye, B.-J. Kim, J. Ryu, J. Y. Lee, J. M. Baik, K. Hong, *Nanoscale* **2015**, *7*, 16189.

[34] J. Chun, J. W. Kim, W. Jung, C.-Y. Kang, S.-W. Kim, Z. L. Wang, J. M. Baik, *Energy*

Environ. Sci. **2015**, *8*, 3006.

[35] G. Zhu, W. Q. Yang, T. Zhang, Q. Jing, J. Chen, Y. S. Zhou, P. Bai, Z. L. Wang, *Nano Lett.* **2014**, *14*, 3208.

[36] J. Chen, G. Zhu, J. Yang, Q. Jing, P. Bai, W. Yang, X. Qi, Y. Su, Z. L. Wang, *ACS Nano* **2015**, *9*, 105.

[37] X. Wang, H. Zhang, L. Dong, X. Han, W. Du, J. Zhai, C. Pan, Z. L. Wang, *Adv. Mater.* **2016**, *28*, 2896.

[38] S. W. Chen, X. Cao, N. Wang, L. Ma, H. R. Zhu, M. Willander, Y. Jie, Z. L. Wang, *Adv. Energy Mater.* **2017**, *7*, 1601255.

[39] W. Seung, H.-J. Yoon, T. Y. Kim, H. Ryu, J. Kim, J.-H. Lee, J. H. Lee, S. Kim, Y. K. Park, Y. J. Park, S.-W. Kim, *Adv. Energy Mater.* **2017**, *7*, 1600988.

[40] J. Chen, H. Guo, X. He, G. Liu, Y. Xi, H. Shi, C. Hu, *ACS Appl. Mater. Interfaces* **2016**, *8*, 736.

[41] C. Keplinger, J.-Y. Sun, C. C. Foo, P. Rothemund, G. M. Whitesides, Z. Suo, *Science.* **2013**, *341*, 984.

[42] Y. Cao, T. G. Morrissey, E. Acome, S. I. Allec, B. M. Wong, C. Keplinger, C. Wang, *Adv. Mater.* **2017**, *29*, 1605099.

[43] C. H. Yang, B. Chen, J. Zhou, Y. M. Chen, Z. Suo, *Adv. Mater.* **2016**, *28*, 4480.

[44] J. Wang, C. Yan, G. Cai, M. Cui, A. Lee-Sie Eh, P. See Lee, *Adv. Mater.* **2016**, *28*, 4490.

[45] C. Larson, B. Peele, S. Li, S. Robinson, M. Totaro, L. Beccai, B. Mazzolai, R. Shepherd, *Science.* **2016**, *351*, 1071.

[46] K. Tian, J. Bae, S. E. Bakarich, C. Yang, R. D. Gately, G. M. Spinks, M. in het Panhuis, Z. Suo, J. J. Vlassak, *Adv. Mater.* **2017**, *29*, 1604827.

[47] D. A. Davis, A. Hamilton, J. Yang, L. D. Cremar, D. Van Gough, S. L. Potisek, M. T. Ong, P. V Braun, T. J. Martinez, S. R. White, J. S. Moore, N. R. Sottos, *Nature* **2009**,

459, 68.

[48] G. O'Bryan, B. M. Wong, J. R. McElhanon, *ACS Appl. Mater. Interfaces* **2010**, *2*, 1594.

[49] S. L. Potisek, D. A. Davis, N. R. Sottos, S. R. White, J. S. Moore, *J. Am. Chem. Soc.* **2007**, *129*, 13808.

Figures

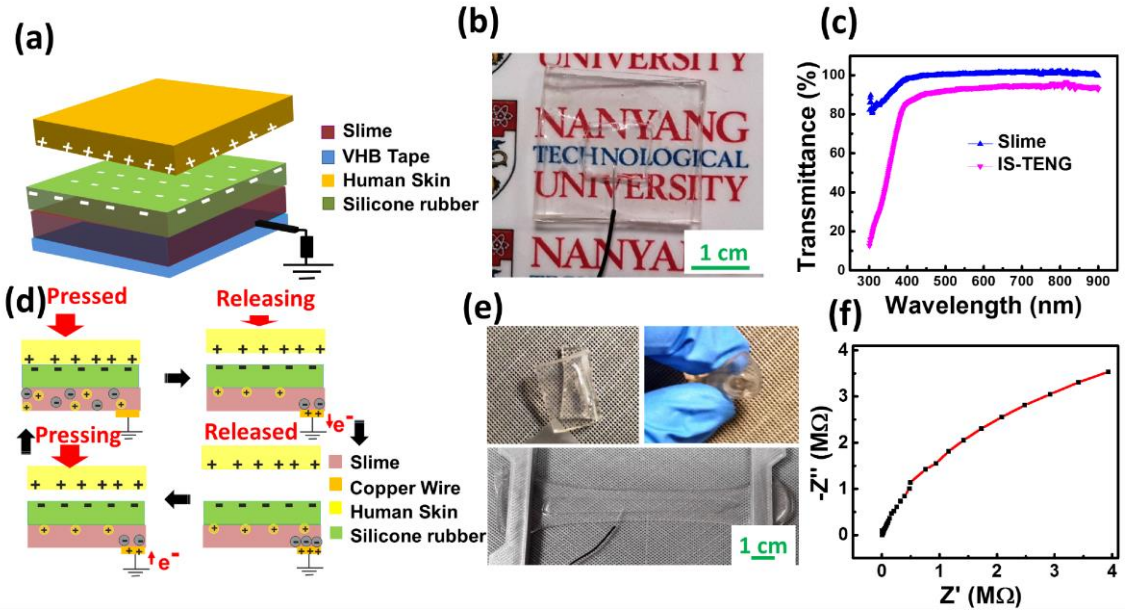

Figure 1. (a) Schematic diagram of the IS-TENG. (b) Digital photo of the highly transparent IS-TENG. (c) Transmittance spectra of the slime (ionic conductor) and the IS-TENG with respect to a glass slide. (d) Schematic illustration of the working mechanism of the IS-TENG. (e) Digital photo of the IS-TENG under various mechanically deformed state such as axial strain upto 700 %, rolled and folded. (f) Electrochemical impedance spectroscopy measurement of the slime (ionic conductor).

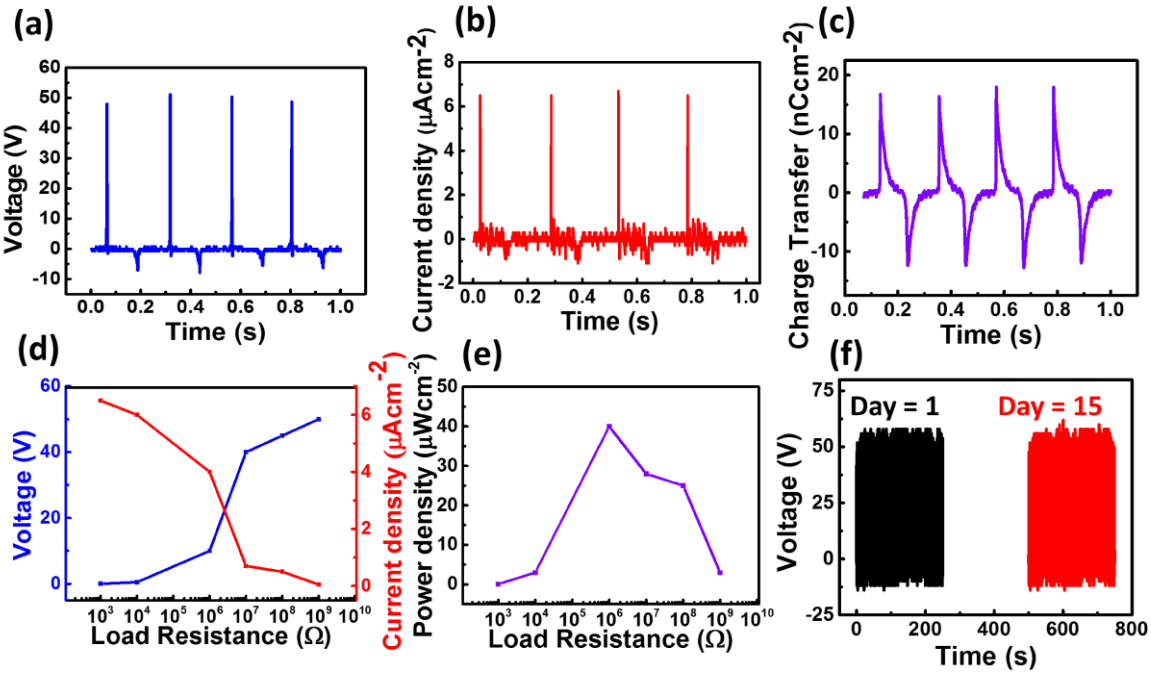

Figure 2. The energy harvesting performance of the IS-TENG upon finger tapping at a force of 10 N exerted at a frequency of 4 Hz. (a) Voltage output (V_{oc}) (b) Current density (I_s) (c) Charge transfer density (σ_T). (d) Variation of voltage and current as a function of load resistance. (e) Variation of power density as a function of load resistance. (f) Stability of the IS-TENG device.

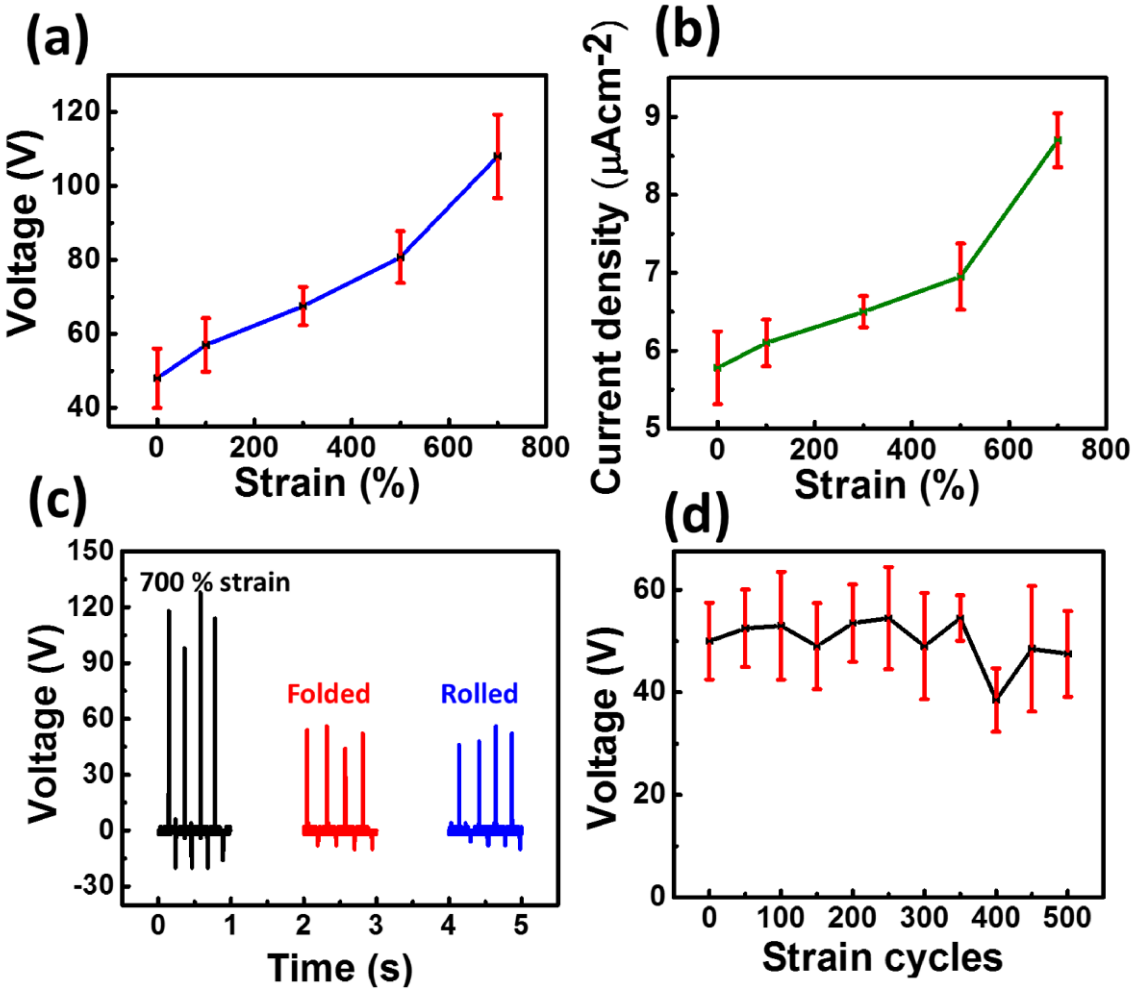

Figure 3. Variation of output performance of the IS-TENG (3 devices, 4 cycles per device) as a function of of axial strain. (a) Voltage output (V_{oc}) (b) Current density (I_s). (c) Voltage output of the IS-TENG at 700 % uniaxial strain, folded and rolled condition with photos of the deformation found in Figure 1e. (d) Stability of the IS-TENG subjected to 500 cycles of dynamic stretching.

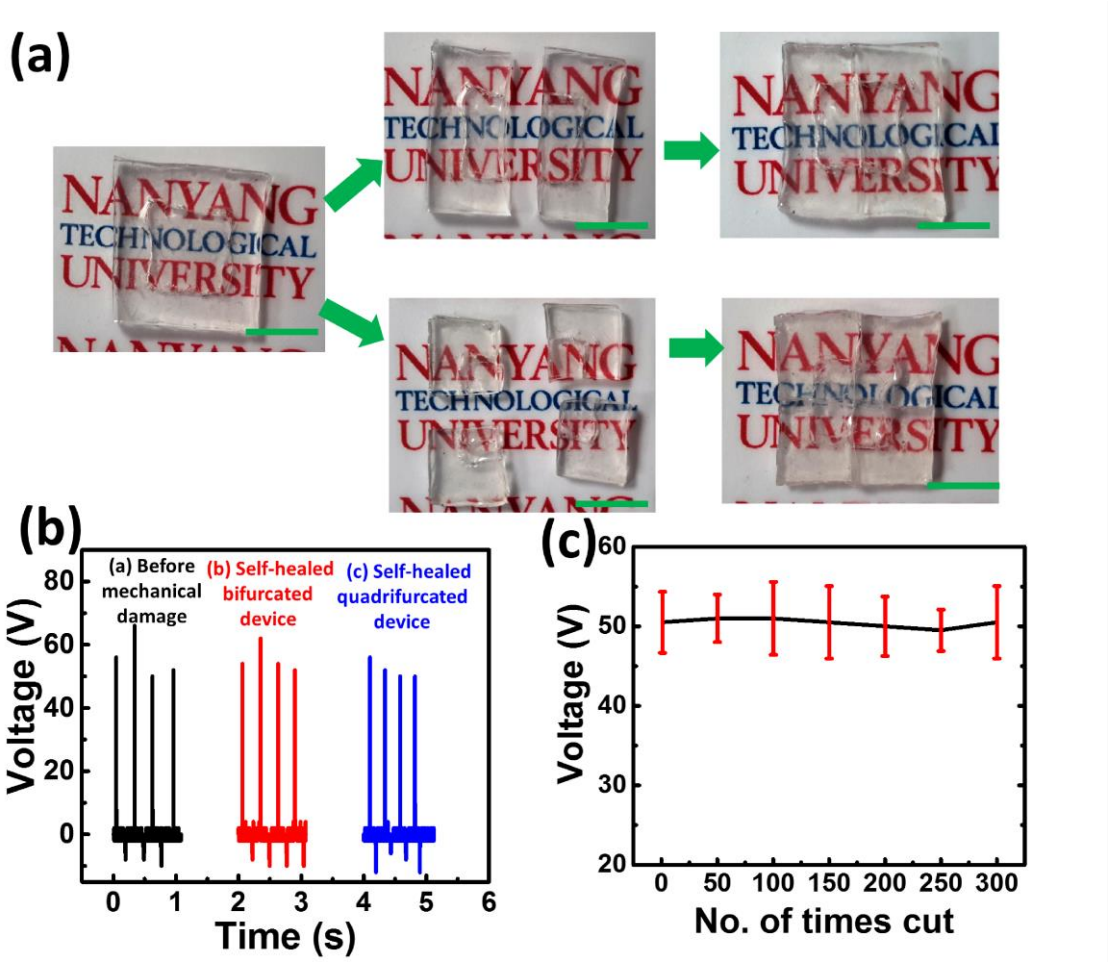

Figure 4. (a) Digital photo of the as-preapared, bifurcated, quadrifurcated and self-healed IS-TENG. Scale bar: 1 cm. (b) Voltage output of the self-healed IS-TENG (c) Stability of the IS-TENG when subjected to multiple bifurcation.

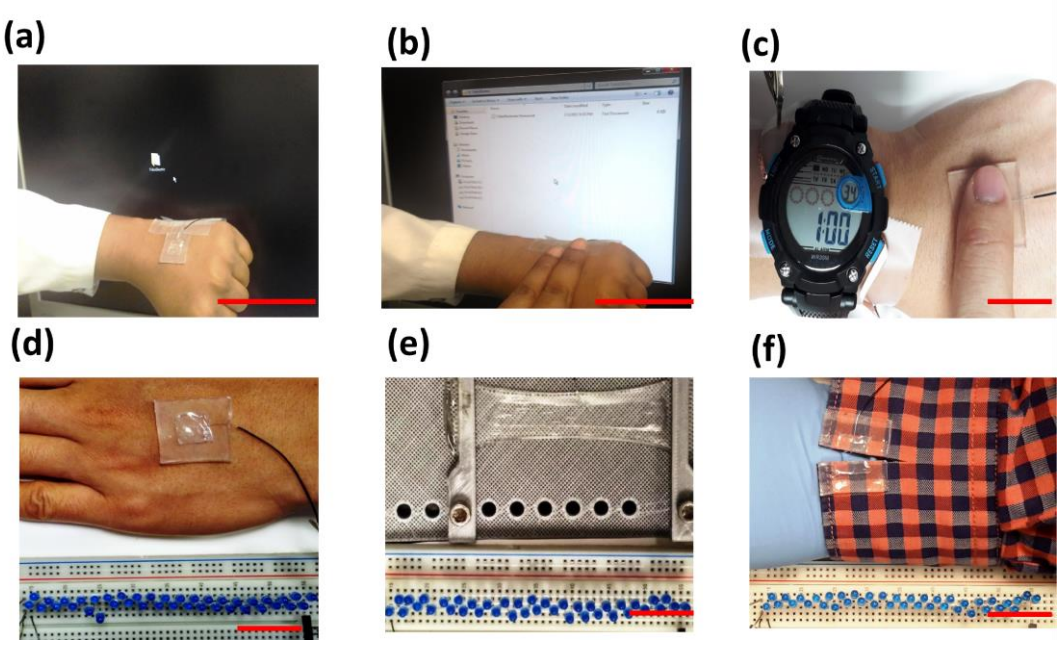

Figure 5. (a) and (b) Digital photo of the IS-TENG as a touch panel to control computer. Scale bar: 10 cm. (c) Digital photo of the IS-TENG to power a digital watch. (d) Digital photo of the IS-TENG attached to the human palm to power 40 LEDs. (d) Digital photo of the IS-TENG under 700 % axial strain to power 40 LEDs. (e) Digital photo of the bifurcated IS-TENG attached to the fabric to power 40 LEDs. Scale bar: 2 cm for (Figure 5c to f).